UCRL-ID-142264

Calibration Results of the EBIT Medium-Energy Flat-Field Spectrometer using the LBL Advanced Light Source

J.K. Lepson, P. Beiersdorfer, G.V. Brown, H. Chen, E.M. Gullikson, M.B. Schneider, S.B. Utter, K.L. Wong

January 17, 2001

U.S. Department of Energy

Lawrence
Livermore
National
Laboratory

This work was performed under the auspices of the U. S. Department of Energy by the University of California, Lawrence Livermore National Laboratory under Contract No. W-7405-Eng-48.

CALIBRATION RESULTS OF THE EBIT MEDIUM-ENERGY FLAT-FIELD SPECTROMETER USING THE LBL ADVANCED LIGHT SOURCE.

Jaan K. Lepson*, Peter Beiersdorfer[+], Gregory V. Brown[+], Hui Chen[+], Eric M. Gullikson[#], Marilyn B. Schneider[+], Steven B. Utter[+], and Keith L. Wong[+].

**Space Sciences Laboratory, University of California, Berkeley*
[+]*Lawrence Livermore National Laboratory*
[#]*Lawrence Berkeley National Laboratory*

ABSTRACT

The relative instrument response function of a flat-field grating extreme ultraviolet spectrometer was determined using the ALS synchrotron source in the wavelength region 40-200 Å. Details of the calibration procedure and results are given in the report.

INTRODUCTION

Accurate analysis of extreme ultraviolet data used in studies of such phenomena as supernova remnants, stellar coronae (Mewe et al. 1995), and Earth-Sun interactions (Warren et al. 1998) requires an accurate and comprehensive catalogue of emission lines in this spectral region. We are using Lawrence Livermore National Laboratory's electron beam ion trap EBIT-II to compile a comprehensive catalogue of wavelengths and intensities for astronomically relevant ions in the EUV region (Beiersdorfer et al. 1999b, Lepson et al. 2000). Accurate determination of relative intensities is a crucial component of this effort, necessitating a calibration of the detection response of our instrument. As part of this effort we used the Lawrence Berkeley Laboratory's Advanced Light Source to calibrate the detector efficiency of the medium-wavelength 1200 line/mm flat-field spectrometer used on EBIT-II (Beiersdorfer et al. 1999a, Utter et al. 1999).

EXPERIMENTAL TECHNIQUE

Data were taken at Lawrence Berkeley National Laboratory's Advanced Light Source beamline 6.3.2. The ALS synchroton produces light over a broad range. A monochromator in the beamline selects light at several harmonics, one of which is selected by a filter. The LLNL spectrometer was bolted to the end of the beamline. See diagram of beamline 6.3.2 in Appendix A. We used a 1,200 line/mm grazing incidence spectrometer developed by Harada and Kita (1980; Nakano et al. 1984) with a 3^{o} an angle of incidence. Readout was taken with a liquid nitrogen cooled CCD camera with a resolution of 1,024 x 1,024 pixels.

Data are acquired by stepping the ALS beamline by a set $\Delta\lambda$ over a given range of wavelengths. Data from a single run of this process are shown in Figure 1.

Several steps are required to complete analysis of the raw data from ALS. First, the data are plotted for each run and the areas of the peaks are calculated using the area function of the program IGOR. Note that the data in Fig. 1 include both first-order (narrowly-spaced) and second-order (widely-spaced) peaks. We took particular care to exclude data where orders overlapped in order to avoid the possibility that higher energies would contribute via higher order to the first order lines we are interested in. Separate analyses were conducted on first and second orders; only the first order was utilized for the purpose of this report.

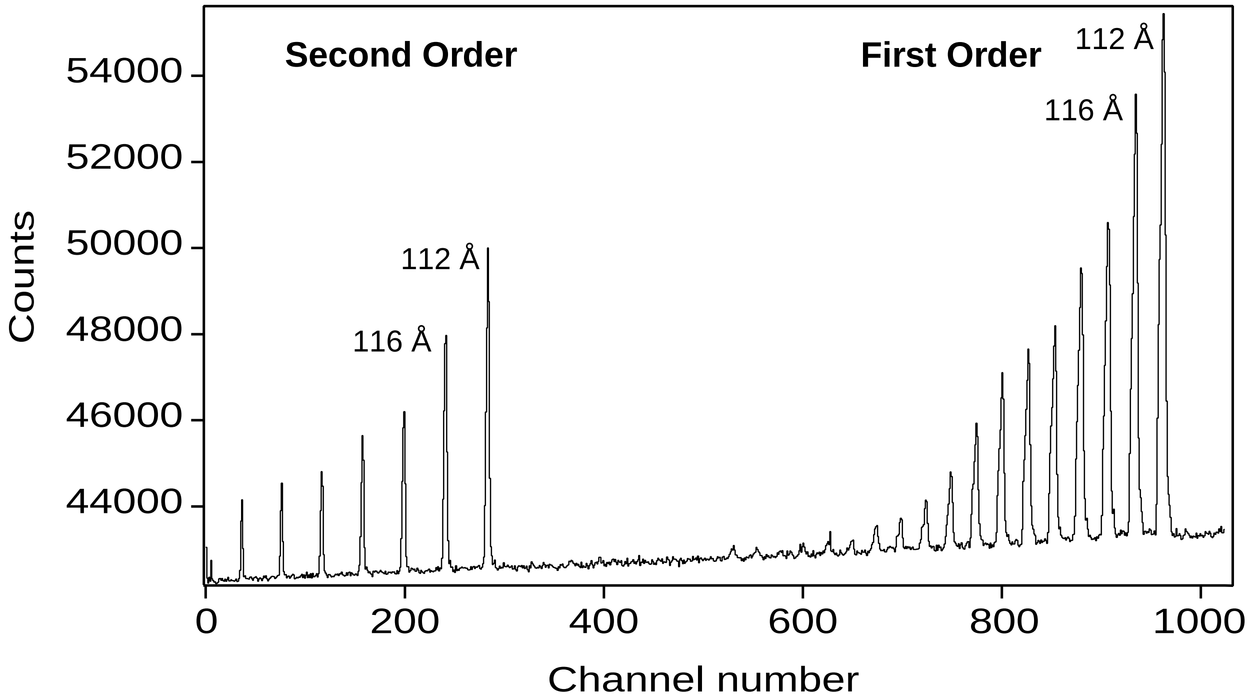

Figure 1. Plot of raw data from ALS using the 1200 line/mm flat-field grating. Peaks begin at 112 Å with a separation of 4 Å.

The second step is to correct for the amount of beam intensity from the ALS. There are two detectors involved that monitor the ALS beamline emission. Detector 1 (Det.1) is upstream near the source, and is constantly monitoring the emission. Detector 2 (Det.2) is near the apparatus and monitors the amount of emission received by the spectrometer, but blocks the sightline and cannot be used when data are taken. Because of this, the correction must be done in two steps. Det.1 can be used while acquiring data, and the relative efficiency of Det.1 and Det.2 can be calculated separately (Det.1/Det.2). The raw data are divided by Det.1 signal and then multiplied by the relative signal strength, Det.1/Det.2. This provides the equivalent of dividing by Det.2 signal. In other words, (Data/Det.1)*(Det.1/Det.2) = Data/Det.2. Figure 2 shows the data set after being corrected for the amount of beam intensity from ALS.

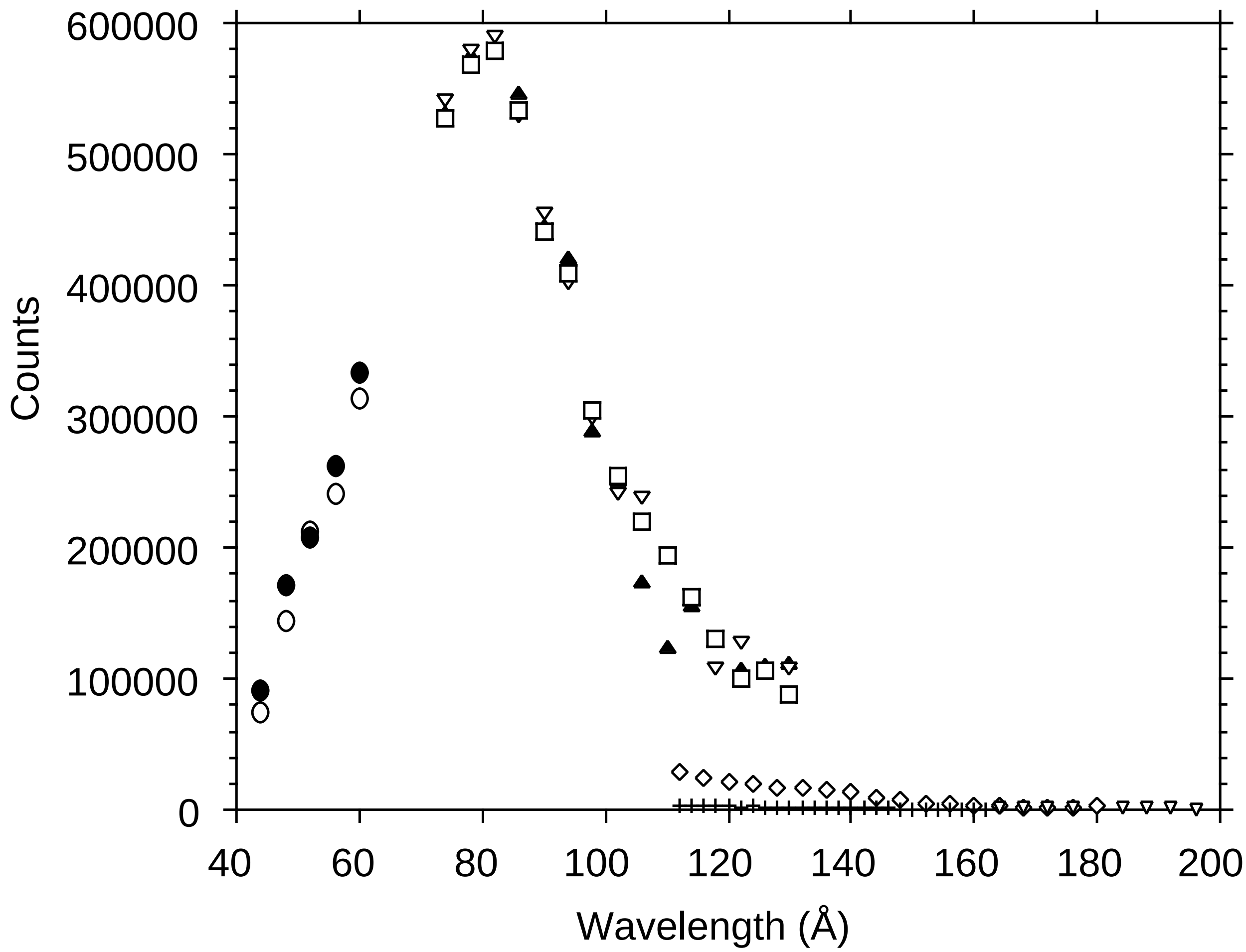

Figure 2. Plot of experimental runs after correction for amount of signal from ALS. Different symbols denote different runs utilized in this analysis.

Because some runs were exposed for longer periods than others, the third step is to correct for differing exposure times. This is done by simple multiplication so that the lines coincide. Figure 3 illustrates the data set after correction for exposure time.

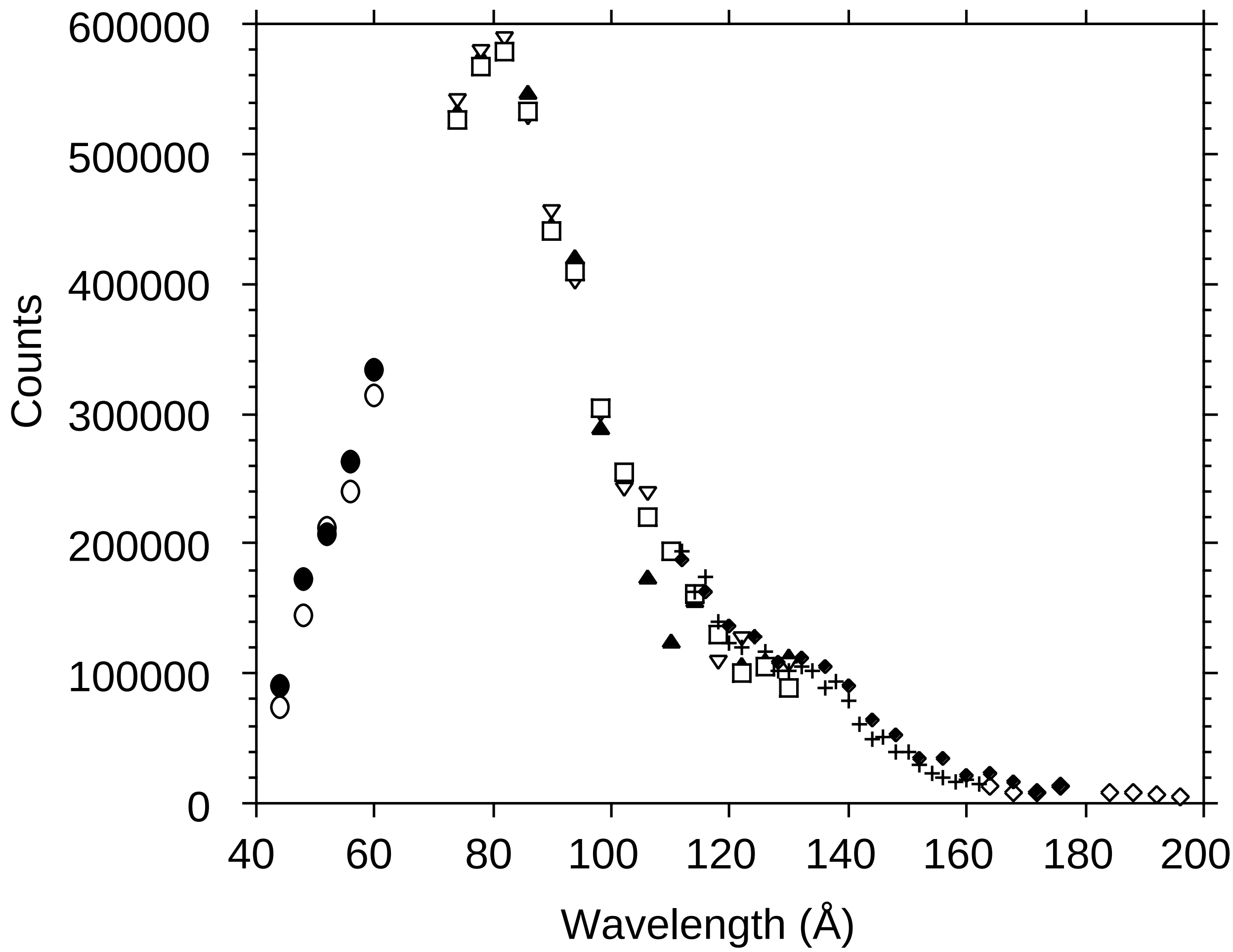

Figure 3. Full data set incorporating all runs used after manual correction for differing exposure times. Different symbols denote different runs utilized in this analysis.

After all this manipulation, the data still do not reflect the true response of the spectrometer. This is because the data are now normalized to the relative efficiency of Det.2. Detector 2 itself does not have a uniform response as a function of wavelength in this wavelength region. To get the actual spectrometer response, we need to adjust for the relative efficiency response of Det.2. This response is shown in Figure 4, as determined by Scholze et al. (2000). They did both a calculation and a measurement; we used their measurement. Our data ranged from 44 Å to 200 Å, a region in which the responsivity function was relatively straightforward. We fit two separate curves to the responsivity function, one from 44 Å to 100 Å, and one from 100 Å to 200 Å.

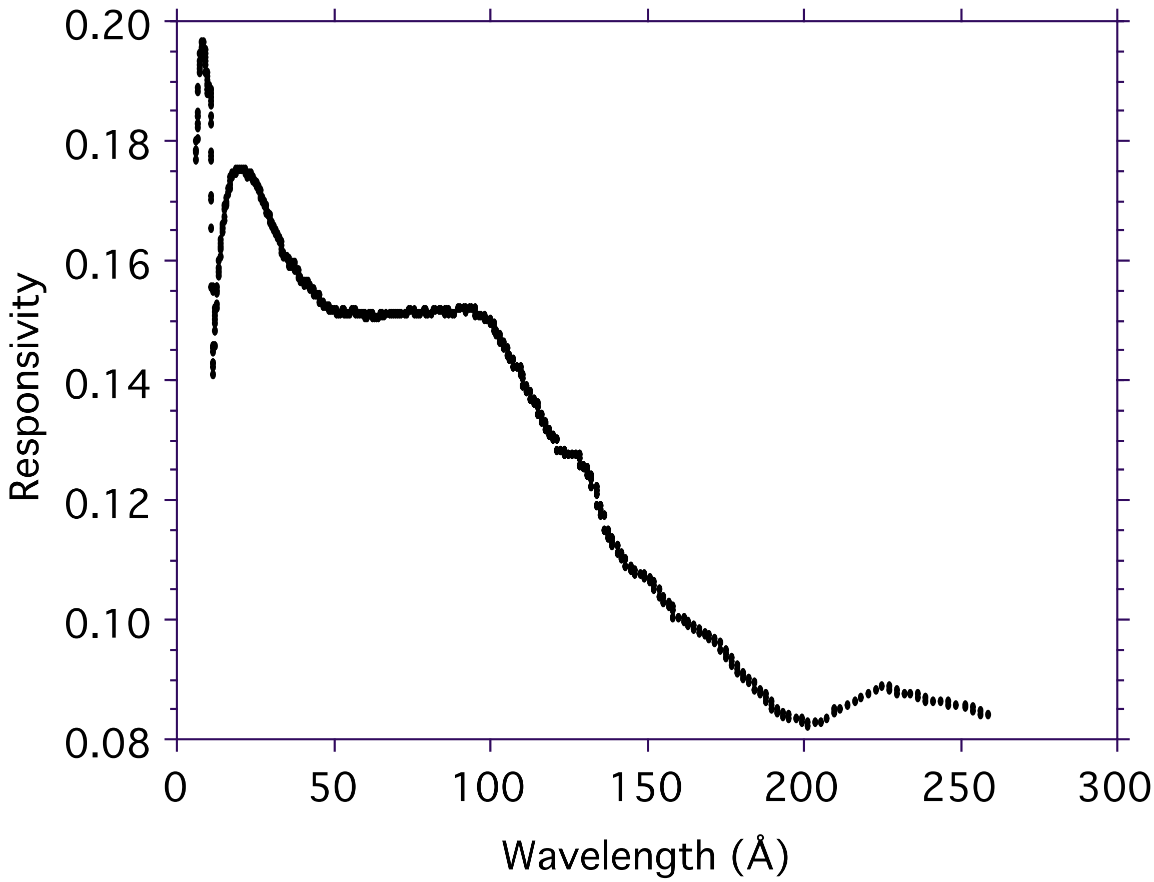

Figure 4. Responsivity function of the ALS diode in Detector 2.

Using the diode response, the detector-corrected data from Figure 3 are then divided by the diode responsivity function derived from Figure 4 to yield the actual spectrometer response. The peak of this data set is then normalized to 1, and is shown in Figure 5. A table of the response data is given in Appendix B. These data can be fit by two polynomial equations, one above 100 Å and one from 100 Å and below. For wavelengths 44 Å $\leq \lambda \leq$100 Å, the response is described by the equation y = -43.9928873 + 3.41086603*x - 0.104141639*x^2 + 0.0015626036*x^3 - 0.0000114067305*x^4 + 0.0000000322854769*x^5. For wavelengths 100 Å < λ < 200 Å, the response is described by the equation y = 25.4867357 - 0.783908447*x + 0.00983263335*x^2 - 0.0000621519248*x^3 + 0.000000196510498*x^4 - 0.000000000247528158**x^5.

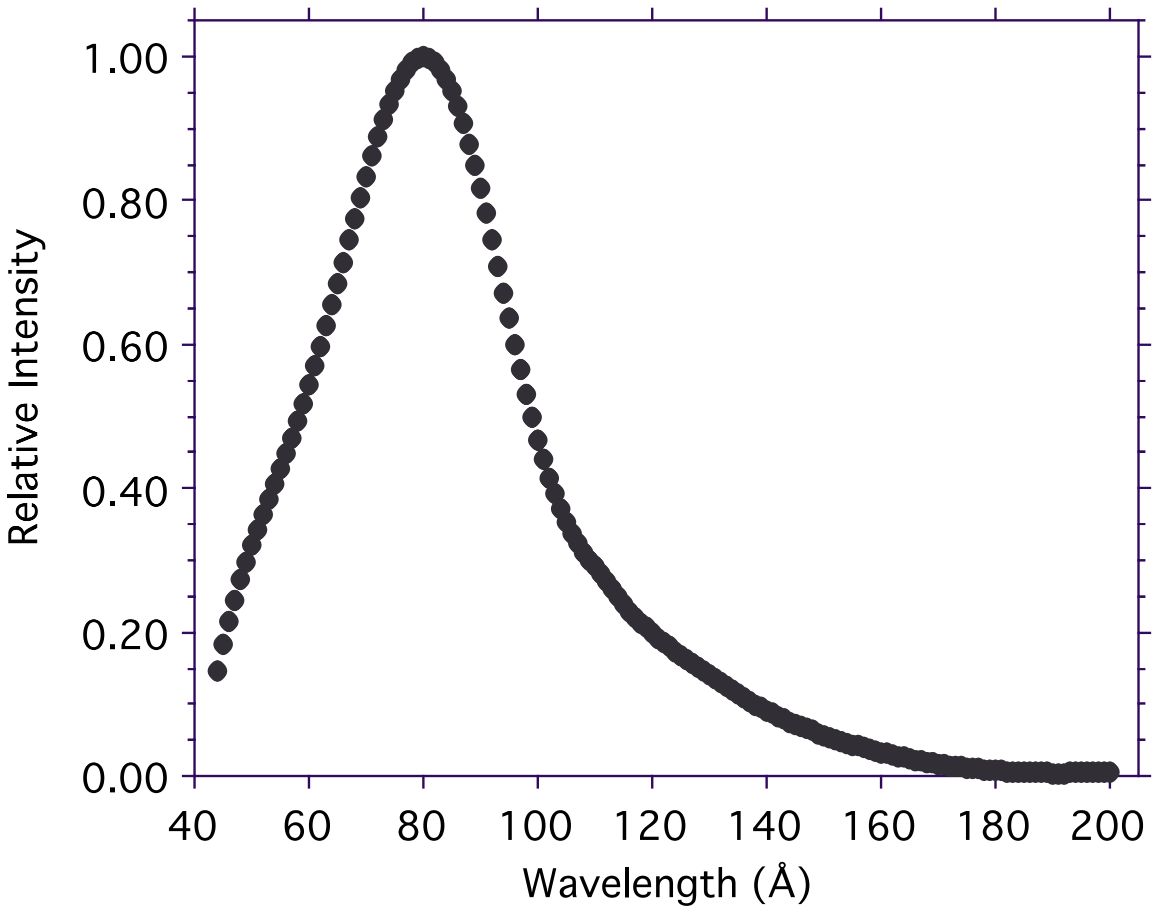

Figure 5. Normalized detector function of the LLNL EBIT 1200 /mm flat field grating spectrometer.

ACKNOWLEDGEMENTS

This work was performed under the auspices of the Department of Energy by the University of California Lawrence Livermore National Laboratory. The work was supported in part by NASA High Energy Astrophysics and an Intra-University transfer agreement between LLNL and the Space Sciences Laboratory at the University of California, Berkeley.

REFERENCES

Beiersdorfer, P., Crespo-López-Urritia, J. R., Springer, P., Utter., S. B., and Wong, K. L., 1999a, *Rev. Sci. Instr.* **70**, 276**.**

Beiersdorfer, P., Lepson, J. K., Brown, G. V., Utter, S. B., Kahn, S. M., Liedahl, D. A., & Mauche, C. W., 1999b, *ApJ* **519**, L185.

Harada, T., and Kita, T., 1980, *Appl. Opt.* **19**, 3987

Lepson, J.K., Beiersdorfer, P., Brown, G. V., Kahn, S. M., Liedahl, D. A., Mauche, C. W., & Utter, S. B., 2000, *RevMexAA* **9**, 137.

Mewe, R., Kaastra, J. S., Schrijver, C. J., van den Oord, G. H. J., & Alkemade, F. J. M., 1995, *A&AS* **296**, 477.

Nakano, N., Kuroda, H., Kita, T., & Harada, T., 1984, *Appl. Opt.* **23** 2386.

Scholze, F., Henneken, H., Kuschnerus, P., Rabus, H., Richter, M., and Ulm, G., 2000, *Nucl. Instr. & Meth. A* **439**, 208.

Utter., S. B., Beiersdorfer, P., Brown, G. V., Clothiaux, E. J., .and Podder, N. K., 1999, *Rev. Sci. Instr.* **70**, 284.

Warren, H. P., Mariska, J. T., & Lean, J., 1998, *J. Geophys. Res.* **103**, 12091

APPENDIX A

Schematic diagram of the ALS Beamline 6.3.2 (www-cxro.lbl.gov/metrology)

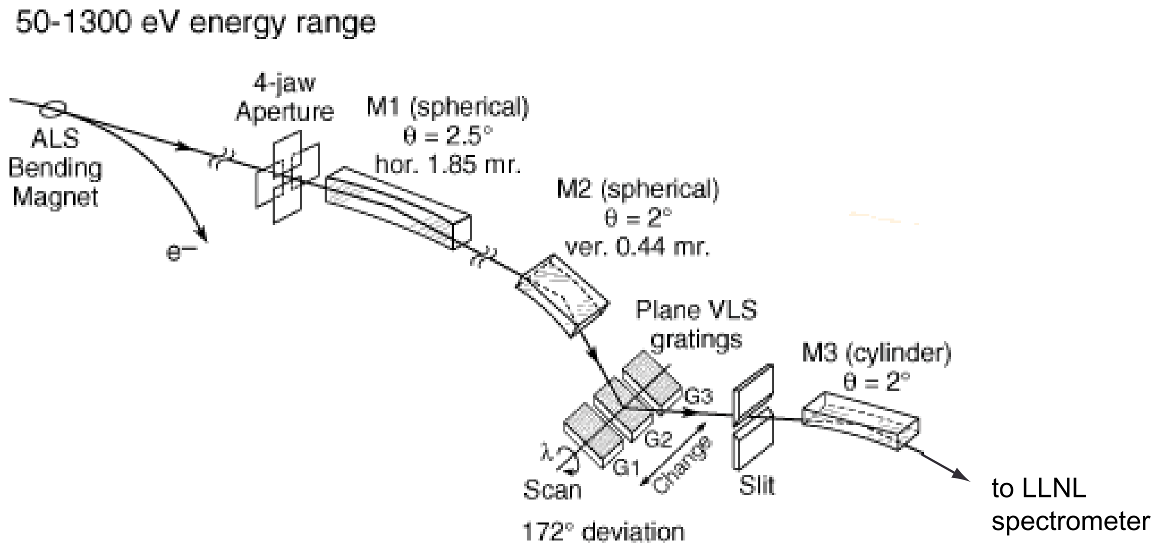

APPENDIX B

Responsivity of the EBIT medium-energy flat-field grating spectrometer by wavelength between 44 and 200 Å.

Wavelength (Å)	Responsivity	Wavelength (Å)	Responsivity	Wavelength (Å)	Responsivity	Wavelength (Å)	Responsivity
44	0.147	81	0.998	121	0.176	161	0.026
45	0.182	82	0.992	122	0.174	162	0.024
46	0.215	83	0.983	123	0.173	163	0.022
47	0.245	84	0.969	124	0.171	164	0.020
48	0.272	85	0.952	125	0.168	165	0.019
49	0.297	86	0.931	126	0.165	166	0.017
50	0.321	87	0.906	127	0.162	167	0.016
51	0.343	88	0.879	128	0.159	168	0.015
52	0.364	89	0.849	129	0.155	169	0.014
53	0.385	90	0.816	130	0.151	170	0.013
54	0.406	91	0.782	131	0.147	171	0.012
55	0.427	92	0.746	132	0.143	172	0.011
56	0.448	93	0.709	133	0.138	173	0.011
57	0.471	94	0.672	134	0.133	174	0.010
58	0.494	95	0.636	135	0.127	175	0.010
59	0.518	96	0.599	136	0.121	176	0.009
60	0.543	97	0.564	137	0.116	177	0.009
61	0.569	98	0.530	138	0.111	178	0.009
62	0.597	99	0.498	139	0.106	179	0.009
63	0.625	100	0.468	140	0.101	180	0.009
64	0.654	101	0.440	141	0.096	181	0.009
65	0.684	102	0.414	142	0.092	182	0.009
66	0.714	103	0.392	143	0.087	183	0.009
67	0.745	104	0.371	144	0.083	184	0.009
68	0.775	105	0.353	145	0.078	185	0.009
69	0.805	106	0.338	146	0.074	186	0.009
70	0.834	107	0.324	147	0.070	187	0.009
71	0.861	108	0.312	148	0.066	188	0.009
72	0.887	109	0.301	149	0.062	189	0.008
73	0.912	110	0.291	150	0.058	190	0.008
74	0.933	111	0.281	151	0.055	191	0.008
75	0.953	112	0.271	152	0.051	192	0.008
76	0.969	113	0.261	153	0.048	193	0.007
77	0.982	114	0.251	154	0.045	194	0.007
78	0.992	115	0.239	155	0.042	195	0.006
79	0.998	116	0.226	156	0.039	196	0.006
80	1.000	117	0.213	157	0.036	197	0.005
		118	0.200	158	0.033	198	0.004
		119	0.187	159	0.031	199	0.002
		120	0.176	160	0.028	200	0.001